Arabian Journal of Chemistry (2021) **14**, 103088

King Saud University

**Arabian Journal of Chemistry**

www.ksu.edu.sa
www.sciencedirect.com

ORIGINAL ARTICLE

# Template-free fabrication strategies for 3D nanoporous Graphene in desalination applications

**T. Tan Vu *, Thi Chien Hoang, Thi Huong Ly Vu, Thu Suong Huynh, The Vinh La**

*School of Chemical Engineering, Hanoi University of Science and Technology, No. 1 Dai Co Viet, Hanoi, Viet Nam*

Received 23 December 2020; accepted 14 February 2021
Available online 23 February 2021

**KEYWORDS**

3D nanoporous Graphene;
Saccharose;
Desalination;
Reduction

**Abstract** For the first time, a novel approach has been developed to fabricate 3D nanoporous Graphene for desalination application. The new approach consists of reducing Graphene Oxide in the presence of saccharose using hydrothermal and microwave combustion routes. The synthesized 3D nanoporous Graphene provides a higher specific surface area than other 3D Graphene synthesized in different ways reported in literatures. In desalination applications, the salt rejection capacity is considerably higher than activated carbon or different carbon-based materials.

The filtered solution conductivity has two orders lower than the feeding solution and stays in the acceptable drinking water range. This excellent result can be explained by the remaining oxygen functional groups, the defects formed during the reduction process, the large specific surface area, and the nanopore of the obtained 3D nanoporous Graphene.



## 1. Introduction

The demand for freshwater has urged the need for seawater desalination (Darre and Toor, 2018). Recently, membrane-based techniques, for example, reverse osmosis (RO), is widely used for seawater desalination (Amy et al., 2016; Goh and Ismail, 2018). However, the RO has a high installation cost, elevated energy consumption, and low desalination capacity. The membrane also suffer fouling problems, flux decline due to the high pressure, rapid degradation, or low stability under acid/alkaline ambient (Tan et al., 2012; Su, 2018).

Recently, nanotechnology provides many options to design desalination membranes containing nanopores with high salt rejection capacity. The nanopores with only a few nanometers, even several angstroms, can permit hydrated ions and reject the salt ions, promising the desalination capacity. Among the materials with nanopores, Graphene and carbon nanotubes are considerably studied for wastewater treatment and desalination purposes (IntechOpen, 2020; Vinh et al., 2019; Tuan et al., 2019, 2020).

Although Graphene material is impermeable, and Graphene with nanopores is considered a promising material for selective membrane applications. The initial research of using Graphene for desalination purposes is molecular dynamics simulations and computational calculations. These works have anticipated that the planar Graphene can allow the water molecules to pass through its nanochannels. The water

* Corresponding author. Tel.: +84 983371922.
E-mail address: tan.vuthi@hust.edu.vn (T.T. Vu).
Peer review under responsibility of King Saud University.

Production and hosting by Elsevier

https://doi.org/10.1016/j.arabjc.2021.103088
1878-5352 

permeability using Graphene as a separation membrane may be mostly higher than that of popular commercial nanofiltration and reverse osmosis (RO) membranes by several magnitudes (Hu and Mi, 2013). The computational simulation shows that the nanoporous Graphene membrane permits the water flow across the defined channels, which is opposite to the slow solution-diffusion water mechanism of RO membranes (Berry, 2013). Several works have demonstrated that the water flow capacity can increase 100 times compared to RO technologies (PUBS, 2021). Two approaches have been applied for Graphene-based membranes are nanoporous Graphene and stacked GO membranes. However, the GO membrane always suffers the swelling effect, which decreases the separation capacity. Therefore, nanoporous Graphene may be the best candidate for water treatment. We already know that the nanochannel pores must be designed with a suitable pore size to avoid the flow of ions. Recently, the control of pore size in material remains one of the drawbacks in the fabrication of membrane. The defects in Graphene sheets, such as the grain boundary or the formed hole after the GO reduction, are considered relevant for the salt rejection (Boretti et al., 2018).

To develop more 2D materials for membrane desalination and ion separation, several 2D materials have been studied for water desalination, such as molybdenum disulfide ($MoS_2$) (Nature, 2021), Phosphorene (Pathania and Gaganpreet, 2021), Boron Nitride (BN) (Liang et al., 2017), and Silicon Carbide (SiC) (Khataee et al., 2017). However, their desalination capacities were studied by only using molecular dynamics simulation and computational calculation. The real salt rejection capacity measured by a membrane made by mentioned 2D materials is still missed. Only experiments have proven the viability of Graphene as 2D materials in water desalination applications.

Recently, porous carbon-based materials provide many industrial fields interest due to their high specific surface area, chemical stability, and low-cost production (Borchardt et al., 2017). Up to now, the pyrolysis of carbonaceous precursors is the primary technique to fabricate porous carbon-based structures (Xu et al., 2017). Among the porous carbon-based materials, the fabrication and application of 3D Graphene-based structures have gained significant attention from many researcher groups (Yang et al., 2015) (Rethinasabapathy et al., 2017). 3D Graphene materials are widely used as chemical adsorbent (Liu and Qiu, 2020; Hiew et al., 2018) , tissue scaffolds (Girão et al., 2020; Li, 2019) energy application (Fan et al., 2015; Venkateshalu and Grace, 2020; Khataee et al., 2017) due to their high porosity properties, high electrical conductivity, and chemical, biological stability.

Template and template-free method are two main synthesis approaches of 3D nanoporous Graphene-based materials (Khataee et al., 2017; Huang et al., 2014; Zhang et al., 2019; Xiong et al. 2019; Vu et al., 2020). For the template method, both hard-templates such silica and polystyrene spheres or metal foams and soft-templates such as polymeric or amphiphilic compounds are widely used to fabricate 3D nanoporous Graphene (Niu et al., 2018; Zhang et al., 2018; Sun et al., 2014). However, the use of hard-templates also involves the elimination step, which could affect the structure of Graphene. Therefore, a template-free approach is modernly used to manufacture of 3D nanoporous Graphene-based materials (Cai et al., 2019; Liu et al., 2019). Currently, the template-free technique is mainly based on the self-assembly of Graphene oxide and its reduction to Graphene under high temperature, forming hydrogel gelation (Ma and Chen, 2014). In addition, there are several methodologies to fabricate 3D nanoporous Graphene, for example, evaporation (Zhang et al., 2017; Yang et al., 2017) , vacuum filtration (Zhao et al., 2020; Ramos Ferrer et al., 2017) , sugar blowing (Venkateshalu and Grace, 2020; Han et al., 2018; He et al., 2020; Wang et al., 2013).

Lately, sugar-blowing is a simple method for fabricating 3D self-supported Graphene (Venkateshalu and Grace, 2020; Wang et al., 2013). The sugar-blowing approach is involved in the controlled heating of glucose in the presence of a facile decomposition compound, for example $NH_4Cl$ (Wang et al., 2013). During the heating process, the glucose is turned into glucose-derived polymers. The formed polymers are transformed into bubbles by the gases released from the decomposition of $NH_4Cl$ (Wang et al., 2013). Subsequently, the graphitization process is needed to convert the bubbles into Graphene membrane walls with mechanically robust, light, and 3D structures.

Taking advantage of the properties of sugar, in this work, we would like to present, for the first time, a new approach for the fabrication of 3D nanoporous Graphene using a combination of saccharose with Graphene Oxide. This new methodology consists of two synthesis steps: hydrothermal treatment and microwave treatment. The mixture of saccharose and Graphene Oxide is treated under the hydrothermal condition to obtain a slurry of Graphene Oxide -sucrose. The slurry will then be treated in the microwave to convert saccharose into bubbles by the gases released from the functional group of Graphene Oxide. The obtained 3D nanoporous Graphene is used as a salt reject membrane for the desalination application. The results are auspicious, showing a novel methodology of salt rejection 3D Graphene membrane, which can be simply scaled up. The product cost is relatively low compared with the traditional method for the fabrication of 3D nanoporous Graphene. Thus, this synthesis methodology could open a new route for the manufacture of salt rejection membrane.

## 2. Experimental

### 2.1. The preparation of Graphene Oxide

Graphene Oxide (GO) is prepared as a precursor for the preparation of 3D nanoporous Graphene. The natural Graphite flake was used as a raw material for the fabrication of GO using modified Hummer methodology (Vu et al., 2020).

In a typical synthesis, a mixture of 10 g of Graphite, 5 g of sodium nitrate, and 250 mL sulfuric acid 98 wt% were homogenously mixed by mechanical agitation. The mixture temperature was regulated to 5 °C. Afterwards, 35 g of potassium permanganate was slowly added to the reaction.

The oxidation process was carried at 40 °C for 2 h to obtain Graphite oxide. The reaction is stopped by pouring gradually 200 mL deionized water. The rest of the potassium permanganate is eliminated by adding 10 mL of $H_2O_2$ (30 wt%). Immediately, the reaction suspension was turned into a yellow-beige color. The manganese oxide formed during the oxidation process can be eliminated by 50 mL of HCl 20%. Finally, the slurry Graphite oxide was neutralized by deionized water. The obtained material was exfoliated by ultrasound

equipment (750 W, 20 min, amplitude 100%). The unexfoliated Graphene Oxide (GO) was separated from the exfoliated GO using a centrifuge at 2500 rpm for 10 min. The GO concentration was calculated by the vacuum evaporation method.

### 2.2. The preparation of 3D nanoporous Graphene

200 mL of GO 5 g/L was mixed with 1 g saccharose at the mass ratio of 1:1. The prepared mixture was placed into a Teflon autoclave and kept at 80 °C for 3 h. The obtained slurry was thoroughly washed with deionized water to remove all the residual impurities, then dried at 60 °C for several hours. Then the product was treated in the microwave for 5 min to obtain the 3D nanoporous Graphene. The final product was denoted as 3D nanoporous Graphene (Fig. 1).

### 2.3. The desalination system

The filter system contains a vertical column and a collecting bottle (Fig. 2). The amount of active filtered material is 0.5 g with an apparent density of 0.06 g/cm$^3$. The filtration process was performed at the standard pressure with a flow rate of 0.6 L/cm$^2$/h. The conductivity efficiency was measured using the Thermo Scientific Eutech Elite PCTS.

The salt rejection capacity was verified by measuring the solution conductivity after filtering a specific salt solution (20 mL). After the filtering process, the filtered conductivity becomes stable, demonstrating the salt rejection capacity keeps constant after the filtration of a certain amount of the salt solution.

### 2.4. Characterization of the samples

The X-ray diffraction (XRD) patterns of the sample were recorded on a Bruker D8 Advance using Cu Kα radiation (λ = 0.15406 nm). The morphology of the sample was examined by scanning electron microscopy (SEM, FEI Quanta FEG 650 model). The Raman spectra were carried out on a micro-Raman spectrophotometer (JASCO Raman NRS-3000).

The $N_2$ isotherm plots were recorded on a Micromeritics ASAP 2020 analyzer. The specific surface area of the material is estimated by the Brunauer–Emmett–Teller (BET) equation. The degasification process was performed at 150 °C and

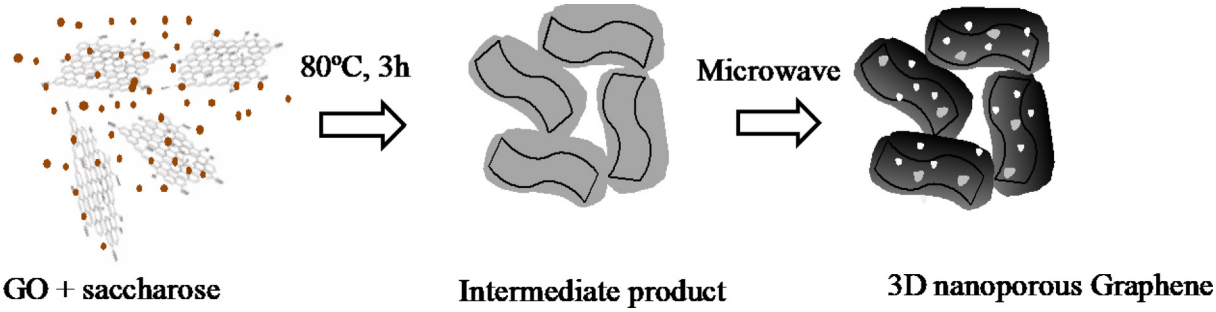


**Fig. 1** The preparation of 3D nanoporous Graphene.

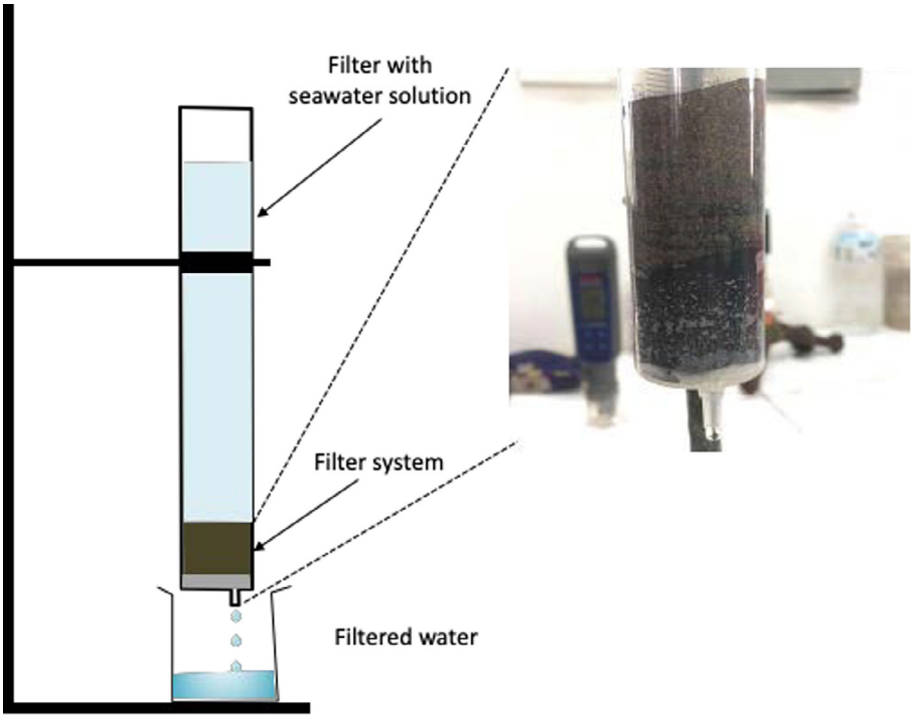


**Fig. 2** The filter system of 3D nanoporous Graphene.

keeped under vacuum condition for 24 h before measurement. The pore size distribution of the material was calculated at $P/P_0 = 0.98$ using the Barrett-Joyner-Halenda (BJH) model.

## 3. Results and discussion

### 3.1. Characterization of the 3D nanoporous Graphene

#### 3.1.1. Scanning electron microscope (SEM) analysis

SEM analysis is widely used to investigate the morphology of the material at the nanoscale (Tan et al., 2020; Tan et al., 2019). Fig. 3 shows the representative high-resolution SEM analysis of the synthesized GO flake (Fig. 3a and b) and the 3D nanoporous Graphene (Fig. 3c and d). The GO layer has a flat structure with transparent morphology before the transformation into a 3D nanoporous Graphene structure.

The successful GO reduction using saccharose can be examined by the surface morphology of the obtained material. Fig. 3c and d show the restacking of Graphene flake, curled and casually aggregated formed 3D structure. The 3D nanoporous Graphene wrinkle assembly shows that GO was wholly reduced in the presence of saccharose.

#### 3.1.2. Transmission electron microscopy (TEM) analysis

The TEM analysis is a fundamental tool for the examination of the morphology structure of the material. Fig. 4 exhibits the TEM images of the synthesized GO. At low-resolution magnification, the GO shows the representative flat 2D struc-

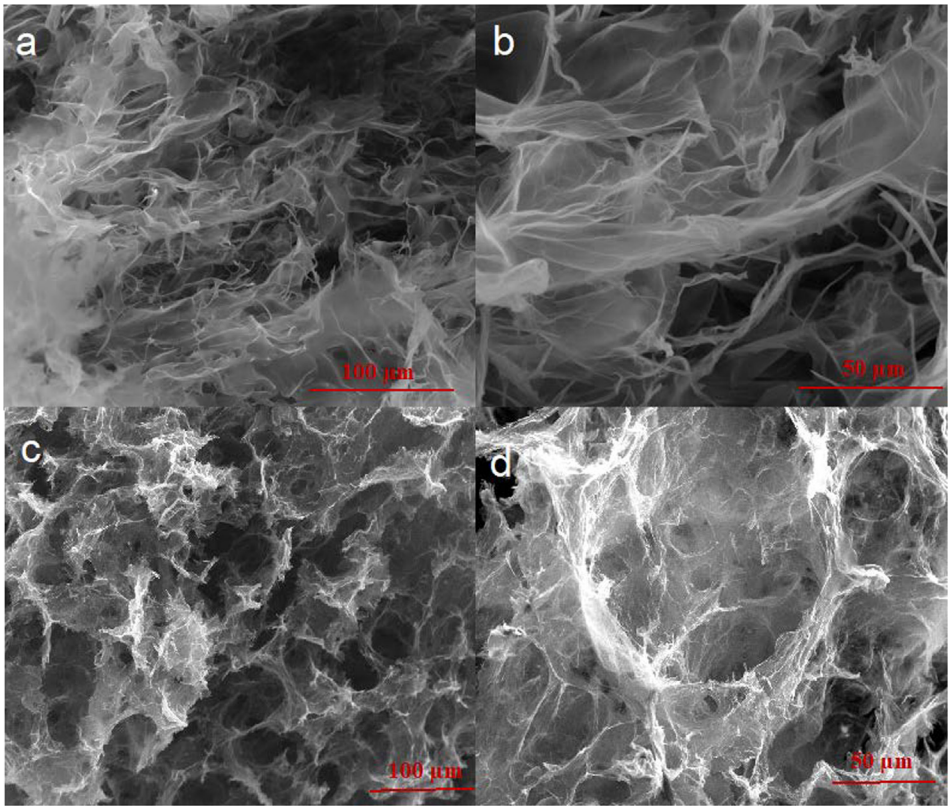


**Fig. 3** The SEM images of Graphene Oxide (3a, 3b); and 3D nanoporous Graphene (3c, 3d).

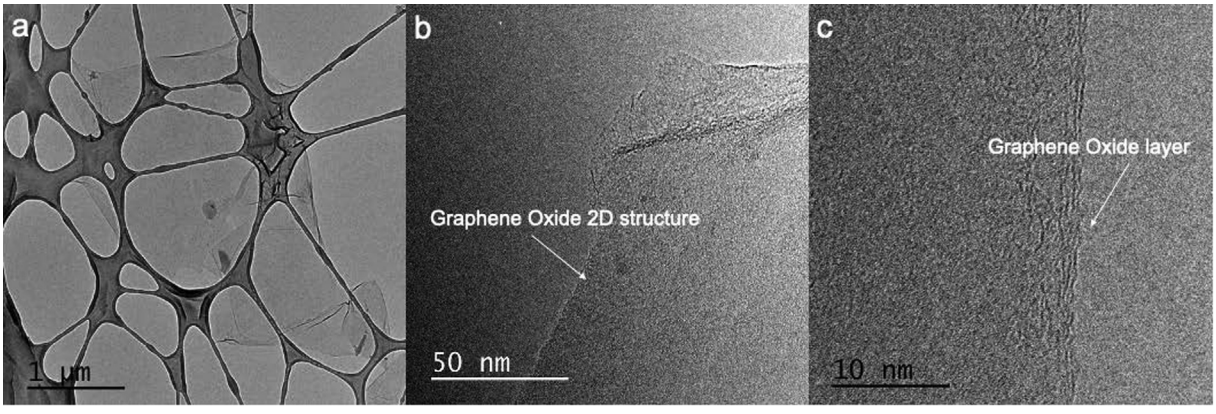


**Fig. 4** TEM images of Graphene Oxide.

ture with the particle size around 10 μm (Fig. 4a). The high-resolution TEM images of Fig. 4b, c display the flat, transparent layer structure with only few GO layers before the reduction with saccharose.

Meanwhile, the low-resolution TEM image of the 3D nanoporous Graphene shows a wrinkled morphology with a 3D structure (Fig. 5a). At higher resolution, the material presents a corrugation structure, and the transparent characteristic of the Graphene layer is still maintained (Fig. 5b). Additionally, the nanopore size on the Graphene surface can be easily observed under a high-resolution TEM image (Fig. 5c). These nanopores were formed during the GO reduction process in the microwave. During the GO reduction process, the saccharose was burnt. Several functional groups of GO were also reduced under the microwave-induced combustion, forming the random nanopore on the surface of Graphene material. The result could make the 3D nanoporous Graphene expose a high specific surface area (Zhang et al., 2019).

### *3.1.3. The X-ray diffraction analysis*

The typical XRD spectra of GO and 3D nanoporous Graphene were measured from 5° to 70°. Fig. 6 shows the XRD of GO at 2θ = 9.76°, corresponding to the (0 0 1) diffraction peak, showing the distance between GO layers is 0.85 nm.

Concurrently, after the reduction process in the presence of saccharose, the peak at 9.76° disappeared utterly, and another

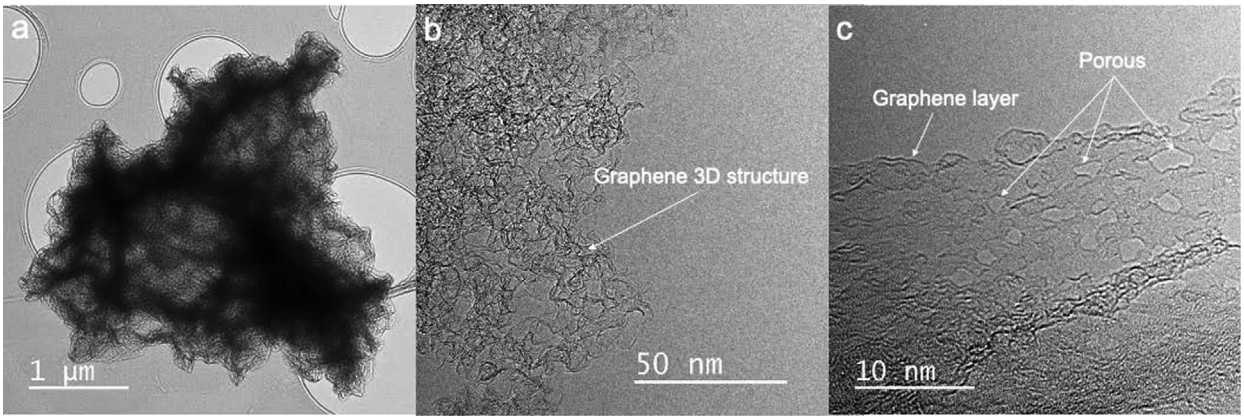


**Fig. 5** TEM images of 3D nanoporous Graphene.

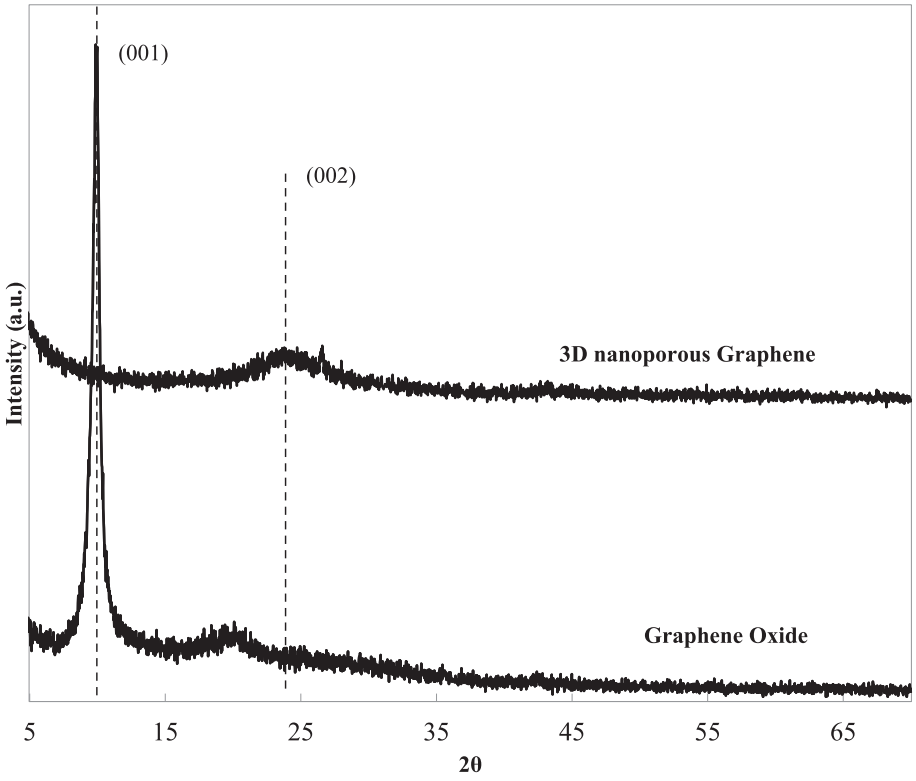


**Fig. 6** XRD pattern of GO and 3D nanoporous Graphene.

peak appeared at 2θ = 23.36°, corresponded to (002) diffraction peak of Graphene-based material (Vinh et al., 2019). The broad peak at 23.36° indicates a short-range order restacking between two Graphene layers, and the distance between them is 0.38 nm (Rivera et al., 2019). The result illustrates that GO was completely reduced during the hydrothermal and microwave treatment.

### 3.1.4. Raman spectroscopy

For the characterization of Graphene-based materials, Raman spectroscopy is an essential technique to determine defect formation. Fig. 7 shows the Raman spectra of both materials GO and 3D nanoporous Graphene.

It can be seen that the G peak at 1621 $cm^{-1}$ is associated with the carbon $sp^2$- hybridization (Ferrari et al., 2006). The D peak at 1352 $cm^{-1}$ is related to the carbon $sp^3$- hybridization or defects on graphene sheets (Vinh et al., 2019). The $I_D/I_G$ intensity ratio is a typical way to evaluate the reduction degree of GO. In Fig. 7, the $I_D/I_G$ ratio of 3D nanoporous Graphene is 1.11; meanwhile, the $I_D/I_G$ ratio of GO is only 0.87. This result demonstrates that GO was wholly reduced during the hydrothermal treatment with saccharose and microwave treatment. The Raman result is totally suited to the XRD, SEM, TEM results. Furthermore, the $I_D/I_G$ ratio can be used to study the spots-like defects in Graphene, which act like nanopores for desalination purposes (Vishnu Prasad et al., 2018).

### 3.1.5. $N_2$ adsorption/desorption measurement

The $N_2$ adsorption/desorption isotherms of both samples GO and 3D nanoporous Graphene are presented in Fig. 8. The isotherms of both materials are very different due to their specific texture. As specified by IUPAC classification, the isotherm of GO corresponds to hysteresis loop H3, which is associated with slit-shaped pores. As well, the isotherm of 3D nanoporous Graphene is related to hysteresis loop H4, which exhibits the structure with narrow slit pores (Cychosz et al., 2017). This representative isotherm endorses the characteristic of mesopores in the 3D nanoporous Graphene (Elma et al., 2020).

Fig. 8 shows that the 3D nanoporous Graphene displays a higher specific surface area (563 $m^2/g$) than the prepared GO (210 $m^2/g$). The preparation process of the material could explain this difference. The 3D nanoporous Graphene is fabricated from the hydrothermal reduction of GO in saccharose presence, and then the reduced material was treated by microwave. The companionship of saccharose on the GO surface during the reduction can avoid the aggregation of the formed reduced GO layers, thus keeping the separation between reduced GO layers (Wang et al., 2012). The saccharose may provide an extension in micropores due to the formation of the pore walls (Park and Kwon, 2020). Besides, the saccharose is almost entirely burnt during the microwave treatment, forming regular pores on the Graphene materials (Schmidt et al., 2017).

Table 1 shows the specific surface area, and average pore diameter of the GO, and 3D nanoporous Graphene.

Fig. 9 displays the Barret-Joyner-Halenda (BJH) pore size distributions of two samples: 3D nanoporous Graphene and GO. The average pore sizes of 3D nanoporous Graphene are 2.10 and 4.95 nm; meanwhile, no specific pore size can be found in the BJH pore size distribution of the GO sample (Table 1). The result of GO can be explained by its textural structure from SEM and TEM analysis. It can be seen that GO has a flat form, and in the powder form, the layers are completely separated with a considerable distance. Therefore, it is challenging to form nanopores in GO materials.

It can be concluded that the 3D nanoporous Graphene is mesoporous material as presented by its characteristic hysteresis loop IUPAC nomenclature and its average pore diameter (Gupta and Khatri, 2017). The average pore sizes are 2.10 and 4.95 nm.

Comparing the result above with the results presented in the literature, we can conclude that the new approach for the

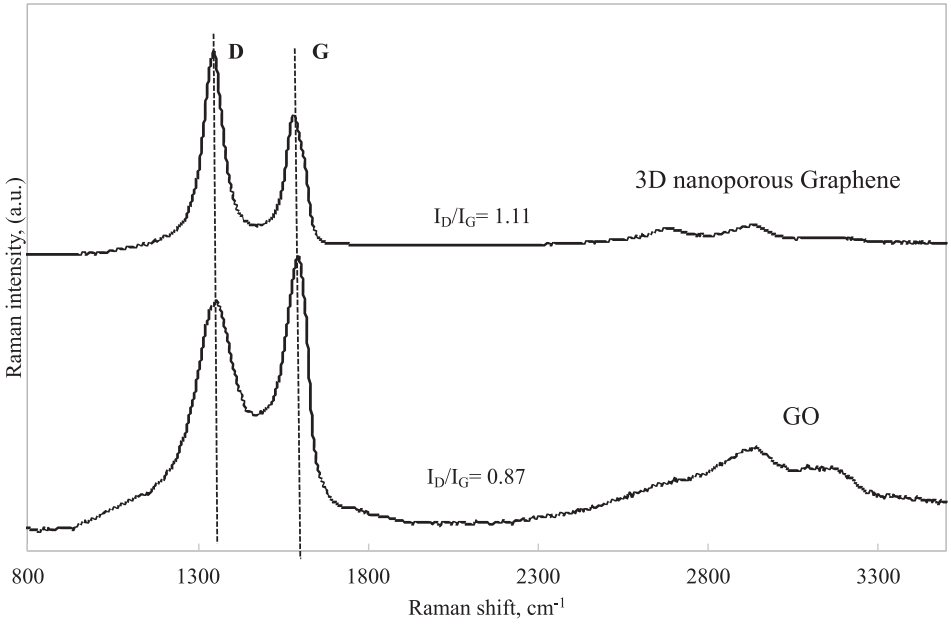


**Fig. 7** Raman spectra of GO and 3D nanoporous Graphene.

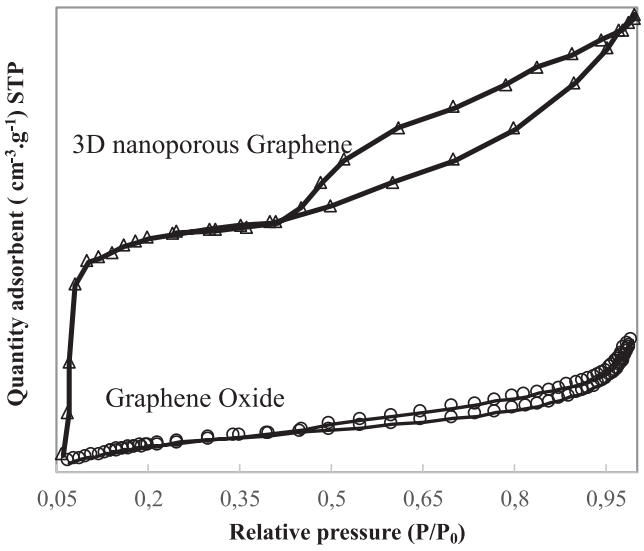


**Fig. 8** $N_2$ adsorption–desorption isotherms of GO and 3D nanoporous Graphene.

**Table 1** Parameters of specific surface area ($S_{BET}$), and the average pore diameter (L).

| Material | $S_{BET}$ ($m^2$/g) | L (nm) |
|---|---|---|
| GO | 210 | – |
| 3D nanoporous Graphene | 563 | 2.10; 4.95 |

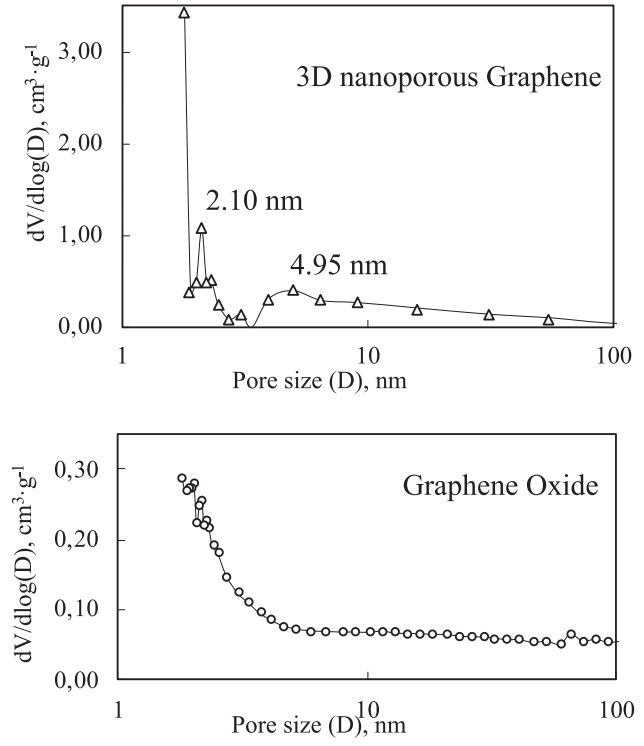


**Fig. 9** Pore width distribution of GO and 3D nanoporous Graphene.

**Table 2** The comparison of specific surface area of different synthesis 3D nanoporous Graphene approaches using saccharose as a precursor.

| Methodology | $S_{BET}$ ($m^2$/g) | Reference |
|---|---|---|
| Hydrothermal and microwave | 563 | This work |
| Microwave synthesis and carbonization | 418 | (Xu et al., 2012) |
| Hydrothermal | 294 | (Nguyen et al., 2012) |
| $CaCO_3$ template | 333 | (Kamedulski et al., 2019) |
| Nickel foam | 412 | (Ping et al., 2017) |
| Chemical deposition | 243 | (3D Graphene, 2020) |

fabrication of 3D nanoporous Graphene via hydrothermal and microwave of this work gives a higher specific surface area than other methodologies reported in the literature. Table 2 shows a comparison of the specific surface area of different synthesis approaches and our work.

### *3.1.6. Elemental analysis*

LECO combustion technique is used to analyze the elemental composition of GO and 3D nanoporous Graphene (Table 3). All the elements are determined by the combustion and pyrolysis process. The result show that the ratio between C and O of GO sample is about 1.1; after the hydrothermal and microwave treatment, the C/O ratio is 7.4. This result demonstrates that GO is entirely converted into 3D nanoporous Graphene after hydrothermal and microwave treatment process (Vu et al., 2020).

### *3.2. Characterization of the filtered salt solution*

The desalination capacity of the material was estimated by measuring the conductivity of the salt solution after passing the membranes (Fig. 10). Firstly, the salt solution flowed through the filter system and its conductivity was monitored.

Fig. 10 shows the conductivity performance of salt solution after passing through the filter system. It can be seen that the solution conductivity decreased by three orders of magnitude after passing the membrane, and afterward increased to reach a stable value. This phenomenon can be explained by the growth of NaCl crystal on the surface of 3D nanoporous Graphene. During the filtration process, the active sites of 3D nanoporous Graphene are saturated by the NaCl crystal. The other salt solution flow may entirely block the 3D nanoporous Graphene nanopores, making the conductivity become established. However, the conductivity of the filtered solution

**Table 3** Elemental analysis of the GO and 3D nanoporous Graphene by LECO combustion.

| Element, wt % | GO | 3D nanoporous Graphene |
|---|---|---|
| C | 49.3 | 87.1 |
| O | 47.1 | 11.7 |
| S | 0.9 | 0.9 |
| H | 2.7 | 0.3 |

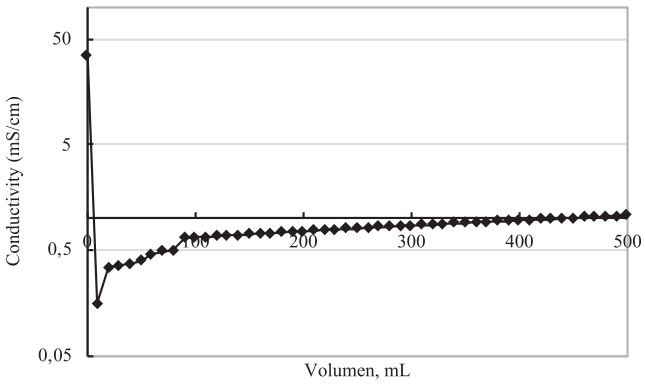


**Fig. 10** Conductivity value of the filtered salt by filtering 0.5 M NaCl solution.

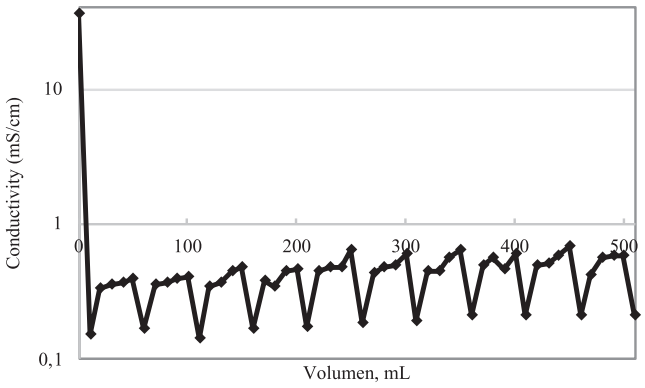


**Fig. 11** Stability salt rejection test after 10 filtration cycles.

is two orders lower than the initial salt solution, and stays in the acceptable range of the tap water. The 3D nanoporous stability was checked by recycling the membrane ten times by washing it with deionized water (Fig. 11). The filtered conductivity value is maintained through 10 times recycling.

The quantity of salt removed from the solution was determined by the conductivity evolution using the following equation (1):

$$m = \int_0^V (C0 - Ct) \times dV \quad (1)$$

where C0 is the initial salt concentration, Ct is the real-time salt concentration determined from the conductivity measurement, and V is the passing solution volume. It is observed that the salt rejection efficiency of the 3D nanoporous Graphene membrane is approximately 71.4 mg/g (after filtering 500 mL of salt solution). The result is considerably higher than that of activated carbon (2–20 mg/g) (Aghakhani et al., 2011), carbon nanotube membrane (5 mg/g), or 3D oxidized Graphene (66.3 mg/g) (Pawar et al., 2016) reported by other researchers.

Fig. 12 shows the microscale analysis of the 3D nanoporous Graphene membranes after the filtration of 0.5 M NaCl solution. It can be seen that salt crystals intertangled on the surface of Graphene. It is already known that the NaCl is highly soluble in water, so there are no suspended particles presented in the solution. The particles found on the surface of Graphene are the NaCl crystal formed during the filtration step. The micro NaCl crystals are grown from unplanned nucleation sites. Fig. 10a shows a lot of small NaCl particles on the surface of the 3D nanoporous Graphene membrane. They are identified by mapping analysis of the used membrane after the filtering process (Fig. 12 c, e). Fig. 12b and d identified the carbon and oxygen distribution of the membrane.

## 4. Conclusions

For the first time, the 3D nanoporous Graphene was fabricated by the reduction of GO in the presence of saccharose via hydrothermal and microwave routes. The SEM and TEM characterizations show that the obtained Graphene presents a wrinkled morphology with a 3D dimensional structure. XRD and LECO analysis reveal that the GO was highly reduced to RGO by combining both hydrothermal and microwave approaches. The 3D nanoporous Graphene synthesized in this work exhibits a higher specific surface area than many other template approaches.

This is the first research that has used 3D nanoporous Graphene synthesized by microwave as a filter material for desalination purposes. The filtered solution has a conductivity two orders lower than the feeding solution and stays in the accept-

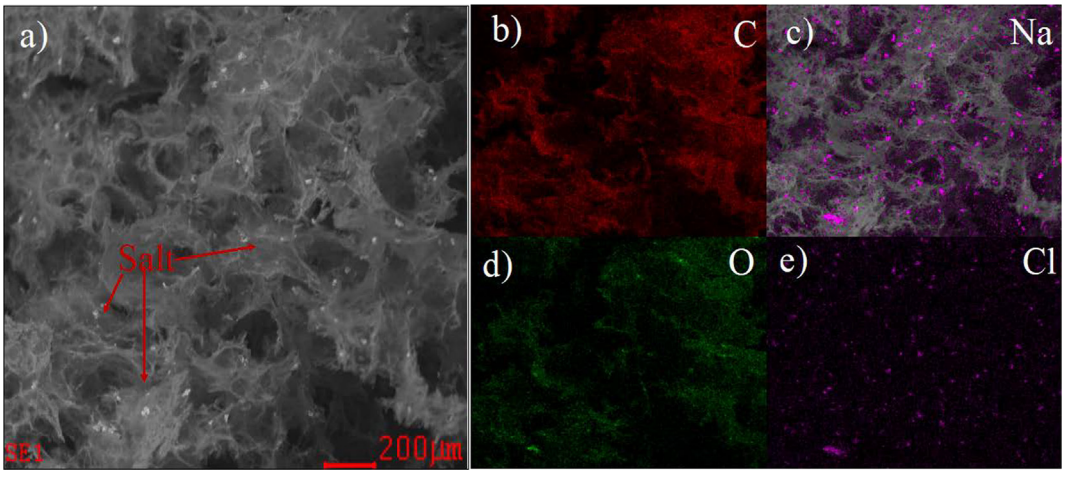


**Fig. 12** 3D nanoporous Graphene membranes after the filtration of 0.5 M NaCl solution.

able range of the drinking water. The result is considerably higher than that of activated carbon and Graphene membrane in another research. This result may differ due to the mesoporous structure of the 3D nanoporous Graphene, its 3D structure, the vacancy defects on the surface of the reduced Graphene material, which could provide a high desalination capacity.

## Declaration of Competing Interest

The authors declare that they have no known competing financial interests or personal relationships that could have appeared to influence the work reported in this paper.

## Acknowledgments

This research is funded by Vietnam Ministry of Education and Training under grant number B2020-BKA-562-22.

## References

3D Graphene Nanostructure Composed of Porous Carbon Sheets and Interconnected Nanocages for High-Performance Lithium-Ion Battery Anodes and Lithium–Sulfur Batteries. ACS Sustain. Chem. Eng. https://pubs.acs.org/doi/10.1021/acssuschemeng.9b00564 (accedido dic. 12, 2020).

Aghakhani, A., Mousavi, S.F., Mostafazadeh-Fard, B., Rostamian, R., Seraji, M., 2011. Application of some combined adsorbents to remove salinity parameters from drainage water. Desalination 275 (1), 217–223. https://doi.org/10.1016/j.desal.2011.03.003.

Amy, G. et al, 2016. Membrane-based seawater desalination: Present and future prospects. Desalination 401. https://doi.org/10.1016/j.desal.2016.10.002.

Berry, V., 2013. Impermeability of graphene and its applications. Carbon 62, 1–10. https://doi.org/10.1016/j.carbon.2013.05.052.

Borchardt, L. et al, 2017. Toward a molecular design of porous carbon materials. Mater. Today 20 (10), 592–610. https://doi.org/10.1016/j.mattod.2017.06.002.

Boretti, A., Al-Zubaidy, S., Vaclavikova, M., Al-Abri, M., Castelletto, S., Mikhalovsky, S., 2018. Outlook for graphene-based desalination membranes. NPJ Clean Water 1 (1). https://doi.org/10.1038/s41545-018-0004-z. Art. no 1.

Cai, X. et al, 2019. 3D graphene-based foam induced by phytic acid: An effective enzyme-mimic catalyst for electrochemical detection of cell-released superoxide anion. Biosens. Bioelectron. https://doi.org/10.1016/j.bios.2018.06.043.

Cychosz, K.A., Guillet-Nicolas, R., García-Martínez, J., Thommes, M., 2017. Recent advances in the textural characterization of hierarchically structured nanoporous materials. Chem. Soc. Rev. 46 (2), 389–414. https://doi.org/10.1039/C6CS00391E.

Darre, N., Toor, G., 2018. Desalination of water: a review. Current Pollut. Reports 4, 1–8. https://doi.org/10.1007/s40726-018-0085-9.

Elma, M. et al, 2020. Carbon templated strategies of mesoporous silica applied for water desalination: A review. J. Water Process Eng. 38, 101520. https://doi.org/10.1016/j.jwpe.2020.101520.

Fan, X., Chen, X., Dai, L., 2015. 3D graphene based materials for energy storage. Curr. Opinion Colloid Interface Sci. 20 (5), 429–438. https://doi.org/10.1016/j.cocis.2015.11.005.

Ferrari, A.C. et al, 2006. Raman spectrum of graphene and graphene layers. Phys. Rev. Lett. 97 (18), 187401. https://doi.org/10.1103/PhysRevLett.97.187401.

Girão, A.F. et al, 2020. 3D Reduced Graphene Oxide Scaffolds with a Combinatorial Fibrous-Porous Architecture for Neural Tissue Engineering. ACS Appl. Mater. Interfaces 12 (35), 38962–38975. https://doi.org/10.1021/acsami.0c10599.

Goh, P.S., Ismail, A.F., 2018. A review on inorganic membranes for desalination and wastewater treatment. Desalination 434, 60–80. https://doi.org/10.1016/j.desal.2017.07.023.

Gupta, K., Khatri, O.P., 2017. Reduced graphene oxide as an effective adsorbent for removal of malachite green dye: Plausible adsorption pathways. J. Colloid Interface Sci. 501, 11–21. https://doi.org/10.1016/j.jcis.2017.04.035.

Han, F., Qian, O., Chen, B., Tang, H., Wang, M., 2018. Sugar blowing-assisted reduction and interconnection of graphene oxide into three-dimensional porous graphene. J. Alloys Compd. 730, 386–391. https://doi.org/10.1016/j.jallcom.2017.09.298.

He, C., Jiang, Y., Zhang, X., Cui, X., Yang, Y., 2020. A Simple Glucose-Blowing Approach to Graphene-Like Foam/NiO Composites for Asymmetric Supercapacitors. Energy Technol. 8 (1), 1900923. https://doi.org/10.1002/ente.201900923.

Hiew, B.Y.Z. et al, 2018. Review on synthesis of 3D graphene-based configurations and their adsorption performance for hazardous water pollutants. Process Saf. Environ. Prot. 116, 262–286. https://doi.org/10.1016/j.psep.2018.02.010.

Hu, M., Mi, B., 2013. Enabling Graphene Oxide Nanosheets as Water Separation Membranes. Environ. Sci. Technol. 47 (8), 3715–3723. https://doi.org/10.1021/es400571g.

Huang, X., Sun, B., Su, D., Zhao, D., Wang, G., 2014. Soft-template synthesis of 3D porous graphene foams with tunable architectures for lithium–O2 batteries and oil adsorption applications. J. Mater. Chem. A 2 (21), 7973–7979. https://doi.org/10.1039/C4TA00829D.

Next-Generation Graphene-Based Membranes for Gas Separation and Water Purifications | IntechOpen. https://www.intechopen.com/books/advances-in-carbon-nanostructures/next-generation-graphene-based-membranes-for-gas-separation-and-water-purifications (accedido nov. 20, 2020).

Kamedulski, P., Ilnicka, A., Lukaszewicz, J.P., Skorupska, M., 2019. Highly effective three-dimensional functionalization of graphite to graphene by wet chemical exfoliation methods. Adsorption 25 (3), 631–638. https://doi.org/10.1007/s10450-019-00067-9.

Khataee, A., Bayat, G., Azamat, J., 2017. Molecular dynamics simulation of salt rejection through silicon carbide nanotubes as a nanostructure membrane. J. Mol. Graph. Modell. 71. https://doi.org/10.1016/j.jmgm.2016.11.017.

Khataee, A., Bayat, G., Azamat, J., 2017. Molecular dynamics simulation of salt rejection through silicon carbide nanotubes as a nanostructure membrane. J. Mol. Graph. Modell. 71. https://doi.org/10.1016/j.jmgm.2016.11.017.

Li, J., 2019. 3D graphene-containing structures for tissue engineering, doi: 10.1016/j.mtchem.2019.100199.

Liang, L. et al, 2017. Computer simulation of water desalination through boron nitride nanotubes. Phys. Chem. Chem. Phys. 19 (44), 30031–30038. https://doi.org/10.1039/C7CP06230C.

Liu, Y., Li, S., Wang, Y., Yang, J., 2019. A template-free synthesis of porous 3D honeycomb-like carbons for supercapacitor electrodes. J. Mater. Sci.: Mater. Electron. 30 (6), 5744–5752. https://doi.org/10.1007/s10854-019-00869-1.

Liu, H., Qiu, H., 2020. Recent advances of 3D graphene-based adsorbents for sample preparation of water pollutants: A review. Chem. Eng. J. 393, 124691. https://doi.org/10.1016/j.cej.2020.124691.

Ma, Y., Chen, Y., 2014. Three-dimensional graphene networks: Synthesis, properties and applications. Nat. Sci. Rev. 2. https://doi.org/10.1093/nsr/nwu072.

Water desalination with a single-layer MoS2 nanopore | Nature Communications. https://www.nature.com/articles/ncomms9616 (accedido feb. 10, 2021).

Nguyen, S.T., Nguyen, H.T., Rinaldi, A., Nguyen, N.P.V., Fan, Z., Duong, H.M., 2012. Morphology control and thermal stability of binderless-graphene aerogels from graphite for energy storage applications. Colloids Surf. A: Physicochem. Eng. Aspects 414, 352–358. https://doi.org/10.1016/j.colsurfa.2012.08.048.

Niu, J., Domenech-Carbó, A., Primo, A., Garcia, H., 2018. Uniform nanoporous graphene sponge from natural polysaccharides as a metal-free electrocatalyst for hydrogen generation. RSC Adv. 9 (1), 99–106. https://doi.org/10.1039/C8RA08745H.

Park, K.-W., Kwon, O.-Y., 2020. Preparation of Novel Mesoporous Silica Using a Self-Assembled Graphene Oxide Template. Sci. Reports 10 (1). https://doi.org/10.1038/s41598-020-63017-4. Art. no 1.

Pathania, Y., Gaganpreet, 2021. Self-passivated nanoporous phosphorene as a membrane for water desalination. Desalination 497, 114777. https://doi.org/10.1016/j.desal.2020.114777.

Pawar, P.B., Saxena, S., Badhe, D.K., Chaudhary, R.P., Shukla, S., 2016. 3D Oxidized Graphene Frameworks for Efficient Nano Sieving. Scientific Reports 6 (1). https://doi.org/10.1038/srep21150. Art. no 1.

Ping, Y., Gong, Y., Fu, Q., Pan, C., 2017. Preparation of three-dimensional graphene foam for high performance supercapacitors. Prog. Natural Sci.: Mater. Int. 27 (2), 177–181. https://doi.org/10.1016/j.pnsc.2017.03.005.

Tunable water desalination across graphene oxide framework membranes - Physical Chemistry Chemical Physics (RSC Publishing). https://pubs.rsc.org/en/content/articlelanding/2014/CP/c4cp01051e#!divAbstract (accedido feb. 08, 2021).

Ramos Ferrer, P., Mace, A., Thomas, S.N., Jeon, J.-W., 2017. Nanostructured porous graphene and its composites for energy storage applications. Nano Convergence 4 (1), 29. https://doi.org/10.1186/s40580-017-0123-0.

Rethinasabapathy, M., Kang, S., Jang, S.-C., Huh, Y., 2017. Three-dimensional porous graphene materials for environmental applications, undefined, 2017. /paper/Three-dimensional-porous-graphene-materials-for-Rethinasabapathy-Kang/96b0f8e01021014d742c5f5d3aabedfe2e299d63 (accedido nov. 22, 2020).

Rivera, L.M., Betancur, A.F., Zarate, D.G., Torres, D.T., Hoyos, L. M., Garcia, A.G., 2019. Reduction and simultaneous doping of graphene oxide to repel LDL in treatment of atherosclerosis disease, arXiv:1902.01850 [cond-mat, physics:physics], feb. 2019, Accedido: ago. 30, 2020. [En línea]. Disponible en: http://arxiv.org/abs/1902.01850.

Schmidt, L., Bizzi, C.A., Rosa, F.C., Cruz, S.M., Barin, J.S., Flores, E. M.M., 2017. Microwave-induced combustion: towards a robust and predictable sample preparation method. New J. Chem. 41 (14), 6902–6910. https://doi.org/10.1039/C7NJ01359K.

Su, Y., 2018. Chapter 1 Current State-of-the-art Membrane Based Filtration and Separation Technologies, pp. 1-13, doi: 10.1039/9781788013017-00001.

Sun, B., Huang, X., Chen, S., Munroe, P., Wang, G., 2014. Porous Graphene Nanoarchitectures: An Efficient Catalyst for Low Charge-Overpotential, Long Life, and High Capacity Lithium-Oxygen Batteries. Nano Lett. 14 (6), 3145–3152. https://doi.org/10.1021/nl500397y.

Tan, C., Lefebvre, O., Zhang, J., Ng, H., Ong, S.-L., 2012. Membrane Processes for Desalination: Overview. Membr. Technol. Environ., 298–330 https://doi.org/10.1061/9780784412275.ch10.

Tan, V.T., Vinh, L.T., Khiem, T.N., Chinh, H.D., 2019. Facile Template In-Situ Fabrication of ZnCo2O4 Nanoparticles with Highly Photocatalytic Activities under Visible-Light Irradiation. Bull. Chem. React. Eng. Cataly. 14 (2). https://doi.org/10.9767/bcrec.14.2.3613.404-412. Art. n.o 2.

Tan, V.T., The Vinh, L., Tu Quynh, L., Thu Suong, H., Dang Chinh, H., 2020. A novel synthesis of nanoflower-like zinc borate from zinc oxide at room temperature. Mater. Res. Express 7 (1), 015059. https://doi.org/10.1088/2053-1591/ab67fa.

Tuan, P.V. et al, 2020. Effects of annealing temperature on the structure, morphology, and photocatalytic properties of SnO2/rGO nanocomposites. Nanotechnology 32 (1), 015201. https://doi.org/10.1088/1361-6528/abac30.

Tuan, P.V., Hieu, L.T., Tan, V.T., Phuong, T.T., Quỳnh, H.T.T., Khiem, T.N., 2019. The dependence of morphology, structure, and photocatalytic activity of SnO2/rGO nanocomposites on hydrothermal temperature. Mater. Res. Express 6 (10), 106204. https://doi.org/10.1088/2053-1591/ab1e12.

Venkateshalu, S., Grace, A.N., 2020. Review—Heterogeneous 3D Graphene Derivatives for Supercapacitors. J. Electrochem. Soc. 167 (5), 050509. https://doi.org/10.1149/1945-7111/ab6bc5.

Vinh, L.T., Khiem, T.N., Chinh, H.D., Tuan, P.V., Tan, V.T., 2019. Adsorption capacities of reduced graphene oxide: effect of reductants. Mater. Res. Express 6 (7), 075615. https://doi.org/10.1088/2053-1591/ab1862.

Vinh, L.T., Khiem, T.N., Chinh, H.D., Tuan, P.V., Tan, V.T., 2019. Adsorption capacities of reduced graphene oxide: effect of reductants. Mater. Res. Express 6 (7), 075615. https://doi.org/10.1088/2053-1591/ab1862.

Vishnu Prasad, K., Kannam, S.K., Hartkamp, R., Sathian, S.P., 2018. Water desalination using graphene nanopores: influence of the water models used in simulations. Phys. Chem. Chem. Phys. 20 (23), 16005–16011. https://doi.org/10.1039/C8CP00919H.

Vu, T.T., La, T.V., Tran, N.K., Huynh, D.C., 2020. A comprehensive review on the sacrificial template-accelerated hydrolysis synthesis method for the fabrication of supported nanomaterials. J. Iran Chem. Soc. 17 (2), 229–245. https://doi.org/10.1007/s13738-019-01764-6.

Vu, T.T., La, T.V., Pham, V.T., Vu, M.K., Huynh, D.C., Tran, N.K., 2020. Highly efficient adsorbent for the transformer oil purification by ZnO/Graphene composite. Arab. J. Chem. 13 (11), 7798–7808. https://doi.org/10.1016/j.arabjc.2020.09.011.

Wang, X. et al, 2013. Three-dimensional strutted graphene grown by substrate-free sugar blowing for high-power-density supercapacitors. Nature Commun. 4 (1). https://doi.org/10.1038/ncomms3905. Art. n.o 1.

Wang, J., Tsuzuki, T., Tang, B., Hou, X., Sun, L., Wang, X., 2012. Reduced Graphene Oxide/ZnO Composite: Reusable Adsorbent for Pollutant Management. ACS Appl. Mater. Interfaces 4 (6), 3084–3090. https://doi.org/10.1021/am300445f.

Xiong, C. et al, ong et al. 2019. The recent progress on three-dimensional porous graphene-based hybrid structure for supercapacitor. Compos. B Eng. 165, 10–46. https://doi.org/10.1016/j.compositesb.2018.11.085.

Xu, Z. et al, 2012. Electrochemical Supercapacitor Electrodes from Sponge-like Graphene Nanoarchitectures with Ultrahigh Power Density. J. Phys. Chem. Lett. 3 (20), 2928–2933. https://doi.org/10.1021/jz301207g.

Xu, F., Wu, D., Fu, R., Wei, B., 2017. Design and preparation of porous carbons from conjugated polymer precursors. Mater. Today 20 (10), 629–656. https://doi.org/10.1016/j.mattod.2017.04.026.

Yang, Z., Chabi, S., Xia, Y., Zhu, Y., 2015. Preparation of 3D graphene-based architectures and their applications in supercapacitors. Prog. Nat. Sci.: Mater. Int. 25 (6), 554–562. https://doi.org/10.1016/j.pnsc.2015.11.010.

Yang, T., Lin, H., Zheng, X., Ping Loh, K., Jia, B., 2017. Tailoring pores in graphene-based materials: from generation to applications. J. Mater. Chem. A 5 (32), 16537–16558. https://doi.org/10.1039/C7TA04692H.

Zhang, H. et al, 2019. High specific surface area porous graphene grids carbon as anode materials for sodium ion batteries. J. Energy Chem. 31, 159–166. https://doi.org/10.1016/j.jechem.2018.06.002.

Zhang, Y., Sun, L., Li, H., Tan, T., Li, J., 2018. Porous three-dimensional reduced graphene oxide for high-performance lithium-

sulfur batteries. J. Alloys Compd. 739, 290–297. https://doi.org/10.1016/j.jallcom.2017.12.294.

Zhang, Y., Wan, Q., Yang, N., 2019. Recent advances of porous graphene: synthesis, functionalization, and electrochemical applications. Small 15 (48), 1903780. https://doi.org/10.1002/smll.201903780.

Zhang, K., Xia, Y., Yang, Z., Fu, R., Shen, C., Liu, Z., 2017. Structure-preserved 3D porous silicon/reduced graphene oxide materials as anodes for Li-ion batteries. RSC Adv. 7 (39), 24305–24311. https://doi.org/10.1039/C7RA02240A.

Zhao, S. et al, 2020. Graphene-based free-standing bendable films: designs, fabrications, and applications. Mater. Today Adv. 6, 100060. https://doi.org/10.1016/j.mtadv.2020.100060.